Flow Distribution Studies Applied to Deep Hydro-Desulfurization

Isabelle Harter,* Christophe Boyer, Ludovic Raynal, Gilles Ferschneider, and Thierry Gauthier

IFP, BP 3, 69390 Vernaison, France

The two-phase flow distribution inside catalytic reactors operating under trickle-flow conditions was qualitatively studied. Three techniques were developed and applied to optimize the two-phase flow distribution through the catalyst bed. First, a computational fluid dynamic (CFD) tool was used to assist in the design of the inlet gas liquid distributor. Second, the corresponding flow inside a catalyst bed, in terms of liquid flow rate and liquid retention, was measured with the two other experimental techniques: a collecting device and a gamma-ray tomography system. These three techniques complement one another; their combined use is of value in the design and testing of reactor inlet distributors.

1. Introduction

European diesel fuel specifications for the year 2005 call for a maximum sulfur content of 50 ppm or even lower in diesel motor fuels. This entails an industry-wide increase in hydrotreating unit performance, an objective that refiners will achieve by modifying existing hydrotreaters or by building new units. These catalytic fixed-bed reactors operate in the trickle-flow regime. At the ultralow levels required, highly reliable reactor designs are essential (effective catalyst utilization, optimum gas/liquid distribution, and low radial temperature differentiation). This paper centers on one of these crucial issues—the gas−liquid flow distribution. It is known that liquid flow maldistribution in industrial hydrotreating reactors is responsible for creating damaging hot spots, which are observed by thermocouple measurements.

A 2.5% flow bypass in a single-bed reactor with a 2 wt % sulfur content feedstock would lead to a product containing at least 500 ppm of sulfur. This distribution problem is important and has already been considered through detailed investigations.[1−3] Dimitrios, Tsangaris, and Dankworth[4] studied gas−liquid distributions by employing a fixed-bed mock-up unit, 560 mm in diameter, equipped at the bottom with a collector divided into 61 sectors. Their results were completed with computational fluid dynamics (CFD) calculations determining the influence of an obstacle on the gas−liquid distribution and the thermal field inside the catalyst bed. Unfortunately, their results were not compared to any experimental or industrial data. Koyama and Nagai[5] conducted cold model experiments in an air−water/glycerin system to investigate the causes of liquid maldistribution. The apparatus was a 300-mm-internal-diameter acrylic column equipped with a liquid distributor at the top and a liquid collector with 33 compartments at the bottom. Recently, Marcandelli et al.[6] reported an experimental investigation of the liquid distribution in trickle-bed reactors and proposed a homogeneity index to assess the radial liquid distribution. One must note that, in all cited studies, neither pressure effects nor temperature effects on the fluid physical properties are mentioned. Thus, experimental studies to date have been conducted under conditions that are not representative of gas−liquid flow under process conditions.

IFP's research center has developed new tools to characterize the flow distribution inside reactors to improve design rules for reactor internals. In this paper, three complementary and powerful techniques are presented. These tools were developed so that fluid physical properties corresponding to real process conditions could be simulated.

2. Hydrotreating Reactor Development Facilities

2.1. General Description. The optimization or development of a new concept for reactor internals follows several steps. First, technological points that might alter the efficiency of the process must be clearly identified. This is possible only through good feedback with data from industrial plants. In the present case, the data used are reactor performance decreases associated with hot spot formation. The chemical reaction, which is strongly exothermic, is principally located inside the liquid phase. In zones where the gas−liquid ratio becomes very high, thermal control via product vaporization becomes limiting, and the temperature increases significantly, thus creating dry zones. A homogeneous liquid flow distribution is essential to avoid this problem and maximize the utilization of the entire catalyst volume.

One of the determining elements to be resolved is control of the gas−liquid feed distribution before it contacts each catalyst bed. This challenge is not straightforward as the ratio between the reactor and inlet pipe cross sections is always in the range of 50−100. Establishing a superior gas−liquid distribution requires new distributor device concepts that include the following elementary functions: gas−liquid predistribution at the reactor inlet, gas−liquid interactions through a distributor, and the flow distribution over the entire bed inlet. Taking into account these different interactions and the operating constraints, these distribution concepts were developed on the basis of engineering knowledge and practical experience. Simulation studies were performed to define the operating conditions under which the conceptual device is valid. This simulation

* Author to whom correspondence should be addressed. Tel.: 33 4 78 02 20 20. Fax: 33 4 78 02 20 09. E-mail: Isabelle.Harter@ifp.fr.

10.1021/ie001143x CCC: $20.00
Published on Web 11/07/2001

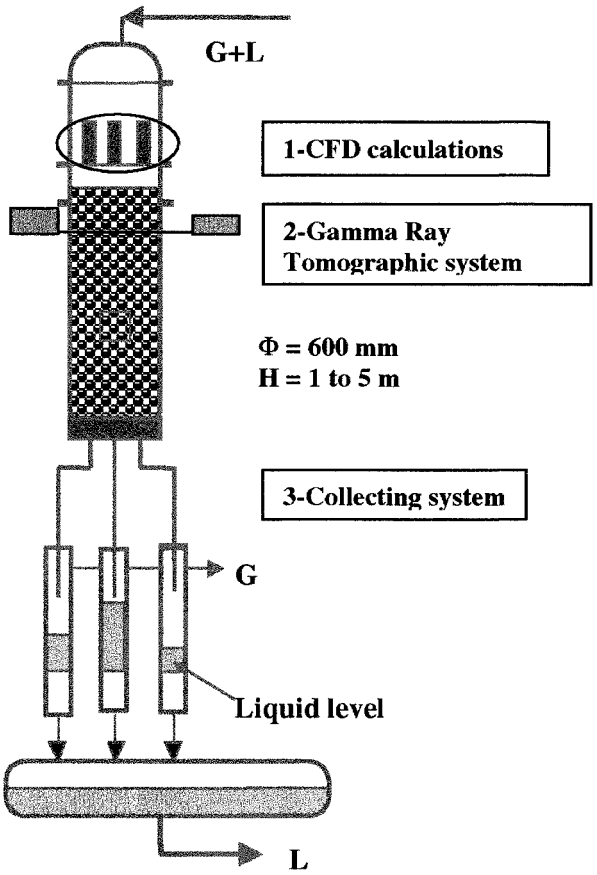

Figure 1. Experimental setup.

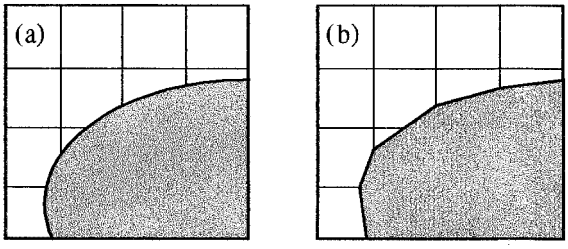

Figure 2. (a) Real shape of the interface and (b) shape calculated using VOF geometric reconstruction scheme.

analysis had to take into account certain force ratios (inertia vs viscosity forces, inertia vs gravitational force, inertia vs interfacial forces, etc.) between industrial reality and the experimental facilities or the mathematical model describing the device. Validation can be perform with two different tools: (1) CFD calculations, providing that the pertinent physical models are available, and (2) experiments on small-scale cold mock-up units when the flow to be simulated is too complex. The last step consists of testing the developed concept on a large, cold flow experimental mock-up unit.

Recently, CFD models have been enhanced significantly, and calculation speeds have greatly increased, so that CFD has become an excellent tool for simulating flow in complex geometries, such as reactor internals. Calculations can be carried out for any geometric complexity and for single-phase and two-phase flows, provided that physical models are available. Nevertheless, the use of this tool becomes possible only when the calculation time is acceptable, i.e., less than a few days. CFD is thus a good link between laboratory experiments, conducted on a small scale with common fluids

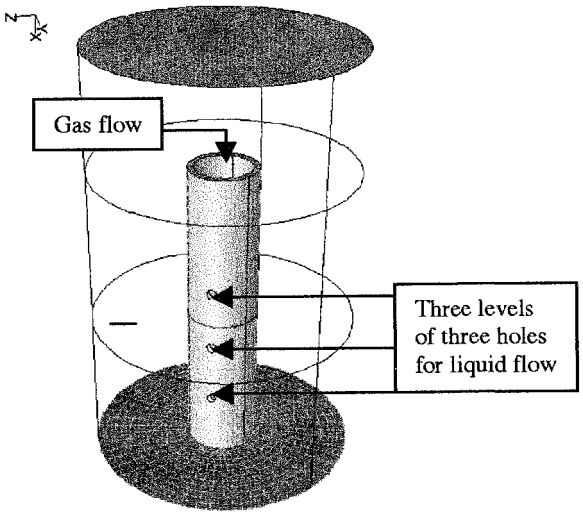

Figure 3. Computational domain and downcomer geometry.

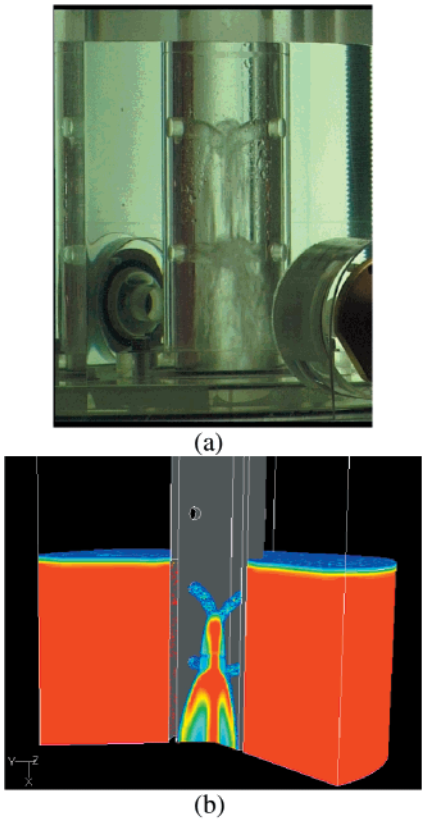

Figure 4. Experimental and numerical flow images inside the downcomer.

(air, water, hydrocarbons, etc.), and industrial operation (large scales, complex fluids, severe pressure and temperature conditions). From this knowledge, we employed this computational tool in our strategy to optimize the industrial distributor devices under hydrotreating conditions.

Experimental studies were carried out on units of two different scales. Small-scale units (typically 1/15th of industrial size) were devoted to studying separately the different flow functions (separation, mixing, spreading) and to testing elementary parts of a device (one downcomer, one bubble cap, etc.) in which all flow functions are examined. Such small-scale units are generally transparent, and the main measurements are based on visualization techniques and classical hydrodynamic

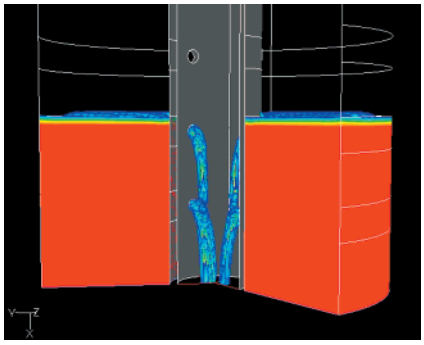

Figure 5. Numerical flow imaging inside the downcomer, fluids under process conditions.

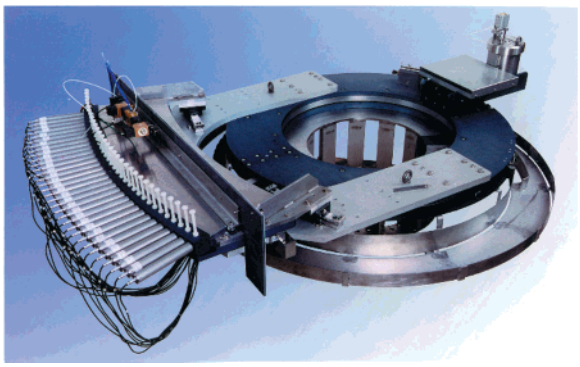

Figure 6. Gamma-ray tomographic system.

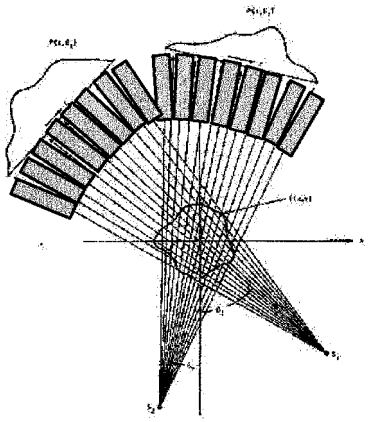

Figure 7. Measured gamma-ray attenuation profiles.

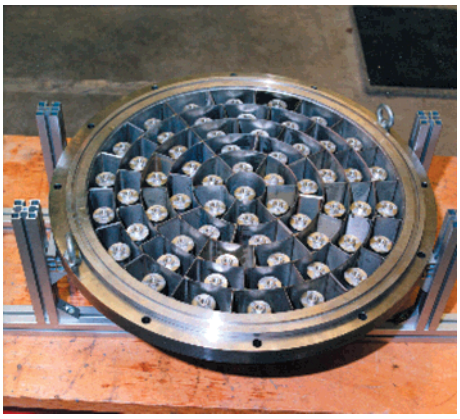

Figure 8. Collecting device.

measurements (pressure, pressure drop, flow rate, phase tracking). Large-scale mock-ups (typically one-fifth of industrial size) were devoted to validating the developed device on a scale representative of the industrial reactor by integrating all coupling between elementary parts of the device.

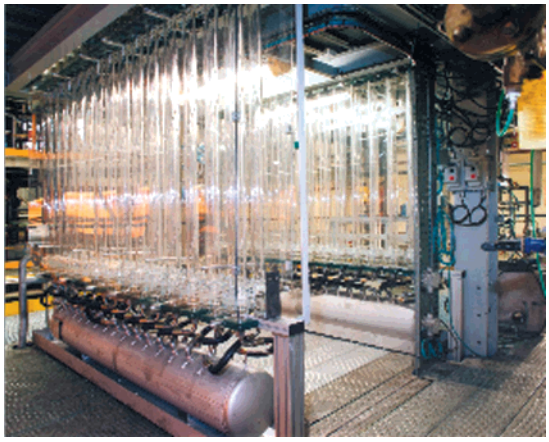

Figure 9. Collecting and measuring tubes.

In this study, the large-scale unit was 5 m high with a 600-mm internal diameter (Figure 1) and was operated at moderate pressures with hydrocarbon (heptane) and nitrogen. The mock-up unit was operated in the trickle-flow regime at pressures between 1 and 4 bar (abs). The admissible liquid flux ranged from 0.35 to 14 kg m^{-2} s^{-1}, and the gas flux ranges from 0.06 to 0.52 kg m^{-2} s^{-1}. Under those conditions, the trickle-flow regime was maintained throughout the bed, according to our visual observations and existing flow regime maps.[7] Specific techniques were developed to measure the liquid flow distribution over the column cross section. Intrusive local measuring techniques were not suitable in the granular catalyst bed medium and under this flow regime. It was difficult to find probes with sensing tips smaller than the intergrain dead volume, so as not to influence fluid flow, but with measuring volumes large enough to ensure a significant space-averaged value. Furthermore, for complete cross-section scanning, a very large number of measurements at different locations was required. As a consequence, nonintrusive techniques were employed. The first technique consists of a gamma-ray tomographic system that provides two-dimensional maps of the liquid retention across the catalyst bed section (see block 2 in Figure 1).

The second technique consists of a collecting system in which the liquid flow rate is measured through 60 sectors at the bed outlet (see block 3 in Figure 1). The techniques are complementary as one gives the local liquid retention inside the bed and the second gives the local liquid flow rate at the bed outlet. Assuming a homogeneous pressure drop across the bed, the local gas and liquid flow rates can be deduced from these two sets of experiments and a two-phase flow model. These systems allow for the quantification of the liquid flow distribution through the bed as a function of bed height, catalyst loading, catalyst properties, operating conditions, and type of tray device used.

2.2. VOF Method. CFD was used to simulate the two-phase flow through a common distributor downcomer (see block 1 in Figure 1 and Figure 3). Because the gas and liquid flows do not interpenetrate the downcomer, a calculation with the volume of fluid (VOF) approach was chosen. The VOF model allows for the computation of two-phase flows where the phases do not mix, i.e., at the gas−liquid interface being clearly

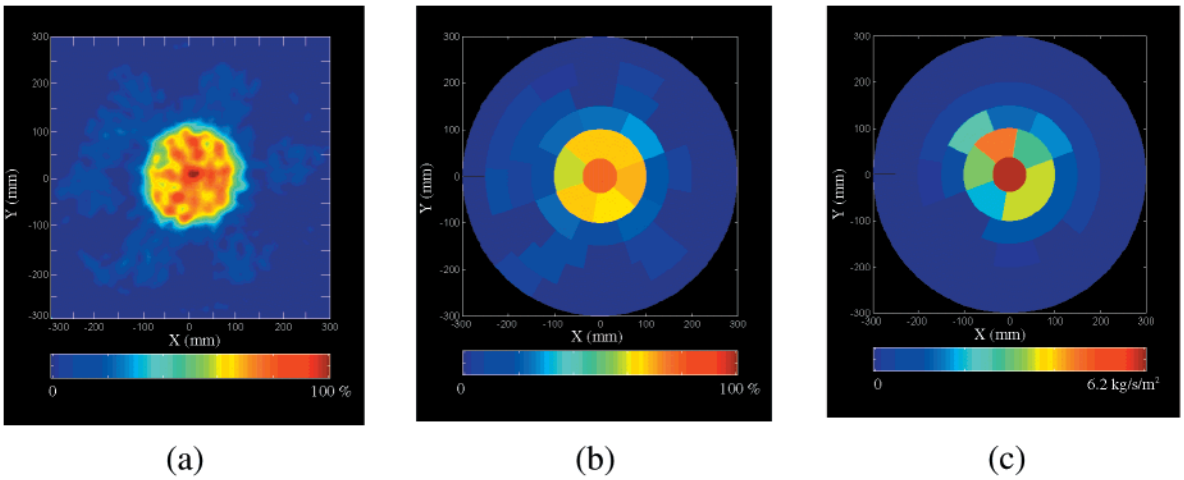

Figure 10. Liquid distribution measurements: (a) liquid retention measured with gamma-ray tomography, (b) liquid retention averaged over each collecting section, (c) liquid flow rate measured at bed outlet by the collecting device. $L = 0.7$ kg m^{-2} s^{-1}; $G = 0.13$ kg m^{-2} s^{-1}.

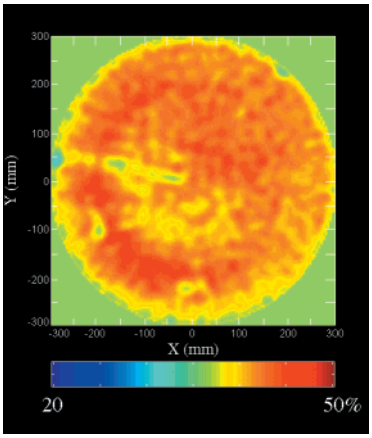

Figure 11. Catalyst bed porosity imaging.

identified. Thus, it is used to calculate the breakup of liquid jets or films sheared by a gas flow[8] or bubble dynamics.[9] In the VOF model, the two fluids share a single set of momentum equations; the tracking of the interfaces is done through the resolution of a transport equation for the volume fraction of one phase. The reconstruction of the interface is accomplished through the use of the geometric reconstruction scheme, which assumes piecewise-linear geometry[10] (Figure 2). Because the Reynolds numbers of the flow are high, the standard $k-\epsilon$ approach was used for turbulence modeling. The commercial code Fluent5.4 was employed for the computations.

Simulations were carried out for chimney geometries that are commonly used to distribute flows on trays (Figure 3). Liquid was injected with a flux of 5 kg m^{-2} s^{-1} at the bottom of the computational domain over an annular surface. Gas was injected with a flux of 0.12 kg m^{-2} s^{-1} at the top round portion of the domain. Considering the geometry, symmetry along two planes at 120° was assumed. Computations were time-dependent with very low time steps, providing good convergence (varying from 10^{-7} to 10^{-3} s mostly depending on the gas-to-liquid density ratio). The calculations were carried out until steady-state conditions were reached, which corresponds to a constant liquid height on the plate and a constant mass flow rate at the exit (central portion of the downcomer). The computational time was about 3−5 days on a R12000 300-MHz processor Octane Silicon workstation.

Figure 4 shows a comparison between the computation results (4b, 2/3 of the domain is shown) and a picture taken in a transparent experimental setup (4a) for identical geometry and flow conditions (water and nitrogen). The superficial velocities employed are representative of those applied industrially. It is experimentally observed that two levels of holes flow through the downcomer. The liquid jets issuing from the second-level holes join at the center axis to form a single jet occupying only a small portion of the downcomer cross section. The latter jet impacts the jets issuing from the first-level holes. This results in a diffuse liquid jet that practically covers the entire exit section. Figure 4b shows the contour of the liquid volume fraction: red corresponds to bulk liquid and blue to the interface. From this figure, one clearly observes the same effect as obtained experimentally. This qualitative agreement implies quantitative agreement as the shape of the jet is directly linked to the local liquid velocity.

From this test case and others not shown, we assumed that the two-phase flow dynamics inside the downcomer is well predicted by CFD calculations, independent of the fluid properties (density, viscosity, and surface tension). This means that similar calculations can be carried out for fluids with physical properties corresponding to hydrotreating process conditions (hydrogen and hydrocarbons under higher pressure and temperature conditions). Figure 5 shows the results obtained from calculations with the same liquid and gas velocities as in Figure 4, but with physical properties corresponding to a standard gasoil under hydrotreating conditions ($T = 340$ °C, $P = 80$ bar).

One observes a dramatic change in the flow configuration. Jets issuing from holes at the same level do not impact each other, as the jet curvature in the downward direction is very strong. The dispersion of the liquid at the exit of the downcomer is consequently much less efficient. This leads to poor wetting of the catalyst bed and will thus negatively impact process efficiency. These calculations show the importance of correctly accounting for process flow properties during development studies. Developing new industrial internals requires testing with the most representative fluids (in terms of viscosity, density, and surface tension). CFD calculations help to define the appropriate operating conditions representative of industrial operation.

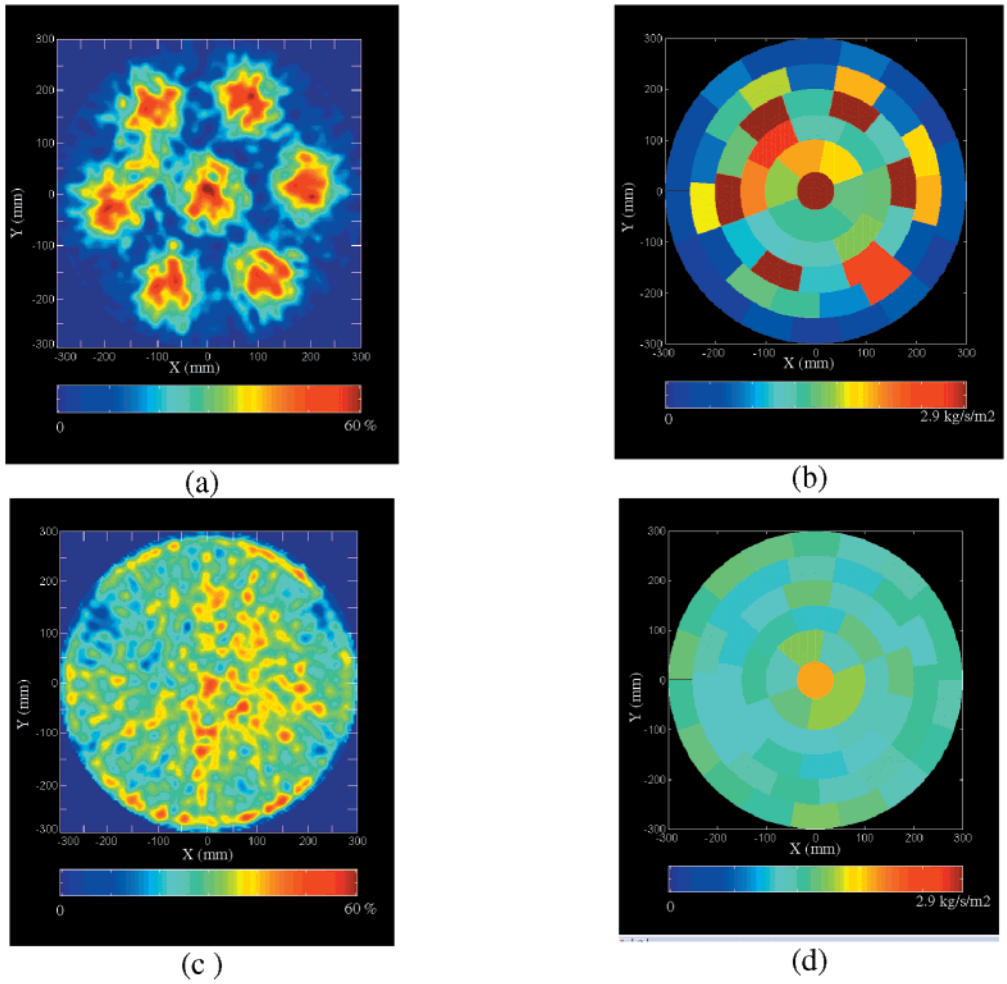

Figure 12. Liquid distribution results obtained with a classical distributing device (a, liquid retention; b, liquid flow rate) and with an optimized inlet distributor (c, liquid retention; d, liquid flow rate). $L = 1.4$ kg m^{-2} s^{-1}; $G = 0.39$ kg m^{-2} s^{-1}.

2.3. Qualification of *G*/*L* distribution inside the Catalyst Bed. *2.3.1. Gamma-Ray Tomographic System.* The liquid retention distribution over a reactor cross section was determined using gamma-ray tomography (Figure 6). This system was composed of a Cs^{137} source with an activity of 300 mCi and 32 detectors consisting of BGO ($Bi_4Ge_3O_{12}$ crystal) photoscintillator transducers. The gamma-ray assembly had a fan beam geometry that could be automatically rotated around the reactor. At each angular position, a photon attenuation profile was measured (Figure 7). After a complete measurement (360°), an attenuation map was constructed using a filtered back-projection reconstruction algorithm.[11] Such systems have been developed for bubble[12] and packed columns.[13]

Because the attenuation is directly proportional to the material density, it is possible to determine the liquid retention from the difference between a measurement in the dry-bed configuration and a measurement with gas−liquid flow across the catalyst bed. In a similar way, the catalyst bed porosity (i.e., intergrain area not occupied by solid material) can be determined from the difference between a dry-bed measurement and a measurement with the empty column. The reconstructed images have a resolution of 128 × 128 pixels. The intrinsic performance of the system was fully studied to examine the different potential errors, including statistical error, dynamic bias due to gas fraction fluctuations, and reconstruction error. The control parameters, measuring time, and scans numbers were optimized.[14] The system was able to measure liquid retention with an absolute accuracy of 3%.

2.3.2. Collector System. To evaluate the flow distribution, a specific collector tray was inserted below the catalyst bed, operating in the trickle phase, to sample gas and liquid from 60 sectors of equal cross-sectional area (Figure 8). Gas−liquid streams from each section at the exit of the column flow through specific gas/liquid separators (Figure 9). Each of the transparent gas/liquid separator tubes is connected at the top to allow for gas disengagement and to control unit bottom pressure. Each tube is equipped with a high-precision calibrated restriction valve at the bottom to maintain a constant liquid level.

After a complete calibration procedure, it is possible to obtain liquid flow rates from individual liquid level measurements and valve opening sections. This results in a two-dimensional map of liquid fluxes or radial liquid flow rate profiles.

2.3.3. Comparison of Measurement Techniques on a Typical Case. The liquid distribution data obtained with both techniques were checked for consistency by comparing results with a typical test. This test case corresponds to a very simple geometry in which the liquid is injected through a 50-mm-diameter tube along the column axis and the gas is injected over the whole bed section. The liquid flow rate is 0.7 kg m^{-2} s^{-1}, and the gas flow rate is 0.13 kg m^{-2} s^{-1}. For a consistent comparison, the distance between the tomographic scanner and the collecting device was reduced to a

minimum length of 70 cm. To reach the same spatial resolution with both systems, the liquid retention results obtained with gamma-ray tomography (Figure 10a) were averaged over segment areas (Figure 10b) corresponding to the collecting device sectors (Figure 10c). The measuring units are different between Figure 10b and 10c, but all of the color maps range from blue for the minimum value (no liquid retention or liquid flow rate) to red for the maximum value of liquid retention or liquid flow rate. It can be seen that the bed areas wetted by liquid detected by the two systems have approximately the same diameter. Furthermore, the amplitude decreases obtained on going from the column axis to the bed periphery are quite comparable for the two measuring systems. First, this confirms that both systems are able to accurately detect the liquid flow amplitude and spatial distribution inside the bed. Second, this result shows that, after the bed inlet layer, there is very little liquid dispersion across the catalyst bed. Thus, poor liquid dispersion at the top of the bed cannot be subsequently recovered.

3. Example of Distribution Device Optimization

Several distributing devices were developed and tested on a 600-mm-diameter cold mock-up unit. Before the liquid distributions inside the bed were tested, the bed porosity was measured using the methodology described in part 3.3.1 (Figure 11). The color map ranges from blue for a porosity of 20% to brown red for a porosity of 50%. This measurement allows for characterization of the bed loading. This can be useful in detecting defective bed loadings that might perturb flow distribution. The distributor efficiency was tested by measuring the liquid distributions under different operating conditions. Typical liquid distribution maps obtained for two distributing devices are shown in Figure 12. A common, basic distributor design in which the gas and liquid flows are injected through seven downcomers was tested (Figure 12a,b). Also, a newer optimized, state-of-the-art distributor was tested to show the performance difference that can be obtained through fluid dynamics development. The operating condition are typical of trickle-flow conditions with a liquid flow rate of 1.4 kg m^{-2} s^{-1} and a gas flow rate of 0.39 kg m^{-2} s^{-1}. The improvement in the liquid distribution obtained with the second distributor is striking. For the classical device, the liquid flows almost straight down from the top inlet to the bed outlet with a very low radial dispersion (Figure 12a and b). The state-of-the-art distributor exhibits a strongly enhanced liquid dispersion and results in a homogeneous liquid distribution inside the bed (Figure 12c) and at the bed outlet (Figure 12d). The standard deviation of the liquid flow distribution measured with the collectors decreases from 70% (classical) to 25% (improved). This new inlet distributor affords an optimized wetting of the catalyst volume, thus limiting potential hot spots and liquid bypass in the column. These factors are a requirement for attaining deep desulfurization levels.

4. Conclusion

Optimization of the gas−liquid distribution in hydrotreating trickle-bed reactors is necessary in view of the low sulfur content imposed by future diesel fuel specifications. A development study was carried out involving both CFD calculations and experiments simulating industrial processes. The VOF approach introduced in the CFD code gives results in good agreement with the observed physical phenomena; furthermore, it shows the importance of operating conditions and fluid properties on flow distribution structure. Local distribution data inside the catalyst bed could be obtained using specific measurement techniques able to detect gas−liquid flow distribution in a granular medium.

These techniques were developed and used on a large scale to evaluate the liquid flow distribution at high resolution. The combination of these different tools affords the possibility of developing and selecting with a high confidence level the most appropriate reactor internals for the attainment of an optimum fluid distribution. Furthermore, the experimental techniques that were developed can be used to investigate the gas−liquid flow structure in the bed and to develop and validate two-phase flow models.[15]

Literature Cited

(1) Ouwerkerk, E. S.; Bratland, A. P.; Hagan, B. L.; Kikkert, J. P.; Zonnevylle, M. C. Performance Optimisation of Fixed Bed Processes. Presented at the European Refining Technology Conference (ERTC), Berlin, Germany, 1998.

(2) Bargsteen Moller L.; Halken, C.; Hansen, J. A.; Bartholdy, J. Liquid and Gas Distribution in Trickle-Bed Reactors. *Ind. Eng. Chem. Res.* **1996**, *35* (3), 926.

(3) Performance Focused Reactor Design to Maximize Benefits of High Activity Hydrotreating Catalysts. Presented at the European Refining Technology Conference (ERTC), London, U.K., Nov 17−19, 1997.

(4) Dimitrios, M.; Tsangaris, D. M.; Dankworth, C. *Impact of Maldistribution on Performance and Safety of Trickle Bed Reactors*; Exxon Research and Engineering Company: Florham Park, NJ, 07928, 1999.

(5) Koyama, H.; Nagai, E.; Torii, H.; Kumagai, H. Japanese Refiner Solves Problems in Resid Desulfurization Unit. *Oil Gas J.* **1995**, 62.

(6) Marcandelli, C.; Lamine, A. S.; Bernard, J. R.; Wild, G. Liquid Flow Distribution in a Trickle Bed Reactor. *Oil Gas Sci. Technol.* **2000**, *55* (4), 407.

(7) Saroha, L. K.; Nigam, K. D. P. Trickle Bed Reactors. *Chem. Eng.* **1996**, *12* (3,4), 207.

(8) Keller, F. X.; Li, J.; Vallet A.; Vandromme, D.; Zaleski, S. Direct Numerical Simulation of Interface Breakup and Atomization. In *Proceedings of the 6th International Conference on Liquid Atomization and Spray Systems (ICLASS-94)*; Begell House, Inc.: New York, 1994; Paper I-8, p 56.

(9) Fan, L. S.; Yang, G. G.; Lee, D. J.; Tsuchiya, K.; Luo, X. Some Aspects of High-Pressure Phenomena of Bubbles in Liquid and Liquid−Solid Suspensions. *Chem. Eng. Sci.* **1999**, *54*, 4681.

(10) *Fluent5 User's Guide*; Fluent Inc.: Lebanon, NH, 1998; Vol. 5.

(11) Kak, A. C.; Slaney, M. *Computerized Tomographic Imaging*; IEEE Press: New York, 1987.

(12) Kumar, S. B.; Moslemiam, D.; Dudukovic, M. P. *Flow Meas. Instrum.* **1995**, *6* (1), 61.

(13) Toye, D. Etude de l'écoulement ruisselant dans les lits fixes par tomographie à rayons X. Ph.D Dissertation, Université de Liège, Liège, Belgium, 1996.

(14) Boyer, C.; Fanget, B.; Legoupil, S. Development of a New Gamma-Ray Tomographic System to Investigate Two-Phase Gas/Liquid Flows in Trickle Bed Reactors of Large Diameter. Presented at the 14th International Congress of Chemical and Process Engineering (CHISA 2000), Prague, Czech Republic, Aug 27−31, 2000; Paper 588.

(15) Carbonell, R. G. Multiphase flow models in packed beds. *Oil Gas Sci. Technol.* **2000**, *55* (4), 417.

Received for review December 30, 2000
Revised manuscript received June 18, 2001
Accepted June 18, 2001

IE001143X